openheart

Anatomical severity of Ebstein's anomaly: a quantitative analysis based on cardiovascular MRI

Giulia Pasqualin,[1,2] Francesco Sturla ,[3,4] Beatrice Cavazza,[1] Lara Tondi,[5,6] Massimiliana Abbate,[1] Francesca Bevilacqua,[1] Federica Torchio,[7] Marina Hughes,[8] Emanuele Micaglio,[9,10] Massimo Lombardi,[5] Pietro Spagnolo,[11] Carlo Pappone,[9,12] Emanuela Angeli,[13,14] Massimo Chessa ,[1,12] Alessandro Giamberti[7,12]

► Additional supplemental material is published online only. To view, please visit the journal online (https://doi.org/10.1136/openhrt-2025-003741).

To cite: Pasqualin G, Sturla F, Cavazza B, *et al*. Anatomical severity of Ebstein's anomaly: a quantitative analysis based on cardiovascular MRI. *Open Heart* 2026;**13**:e003741. doi:10.1136/openhrt-2025-003741

Received 19 September 2025
Accepted 15 December 2025

For numbered affiliations see end of article.

Correspondence to
Dr Francesco Sturla; francesco.sturla@grupposandonato.it

ABSTRACT

Background Ebstein's anomaly (EA) exhibits significant anatomical and clinical heterogeneity, warranting a systematic approach to risk stratification. While the Carpentier classification (CC) is commonly employed for qualitative disease assessment, there is increasing interest in quantitative imaging parameters to personalise monitoring strategies and therapeutic interventions. We sought to evaluate the association between cardiovascular magnetic resonance (CMR) parameters, CC and symptoms of heart failure (HF). Also, we investigated whether CMR-derived markers may predict the need for bidirectional cavopulmonary anastomosis (BCPA) and the occurrence of haemodynamic complications or significant right ventricular (RV) dysfunction in the postoperative stay.

Methods This retrospective study evaluated consecutive patients diagnosed with EA undergoing 1.5T CMR acquisition at a tertiary care centre. CC and quantitative indices were extracted from steady-state free precession sequences.

Results In a total population of 60 patients (53% male, median age 22 years), CMR parameters most strongly associated (p<0.001) with CC included indexed displacement of the septal (SLDi) and inferior (ILDi) leaflets, Ebstein valve rotation angle, functional RV ejection fraction, indexed atrialised RV end-diastolic volume and the ratio of either atrialised or functional RV to anatomical RV. Decreasing left ventricular ejection fraction (OR 0.85, 95% CI 0.75 to 0.97, p=0.01) and increasing ILDi (OR 1.05, 95% CI 1.00 to 1.10, p=0.04) emerged as the most prominent variables associated with HF symptoms. Additionally, ILDi was significantly linked to the need for BCPA (OR 1.15, 95% CI 1.03 to 1.28), the occurrence of haemodynamic complications (OR 1.09, 95% CI 1.01 to 1.18) and significant RV dysfunction in the postoperative stay (OR 1.08, 95% CI 1.01 to 1.17).

Conclusions Quantitative CMR indices proved to be effective in distinguishing between Carpentier classes and they may be valuable in an integrated CMR-based approach to assess EA severity. Among these, ILDi reflects both the extent of tricuspid valve abnormality and RV atrialisation and may serve as a useful metric in guiding personalised therapeutic strategies.

WHAT IS ALREADY KNOWN ON THIS TOPIC

⇒ Ebstein's anomaly is a heterogeneous congenital malformation with variable anatomical severity traditionally assessed qualitatively. Cardiovascular MR (CMR) provides accurate chamber quantification, but validated quantitative indices for grading severity and guiding surgical planning remain limited.

WHAT THIS STUDY ADDS

⇒ This study identifies inferior leaflet displacement index (ILDi) and Ebstein valve rotation angle (EVRA) as robust CMR-derived markers associated with Carpentier class, heart failure symptoms and, exploratorily, surgical outcomes. It demonstrates the feasibility of a quantitative, CMR-based assessment framework for Ebstein's anomaly.

HOW THIS STUDY MIGHT AFFECT RESEARCH, PRACTICE OR POLICY

⇒ Incorporating CMR-derived indices such as ILDi could refine preoperative risk stratification and help tailor therapeutic strategies in Ebstein's anomaly. These findings provide a rationale for multicentre validation studies and may inform future consensus recommendations on imaging-based management.

INTRODUCTION

Ebstein's anomaly (EA) is a congenital malformation characterised by impaired delamination of one or more leaflets of tricuspid valve (TV) to the right ventricular (RV) endocardium. Leaflet adherence to the parietal wall may be direct, manifesting as linear or hyphenated defect, or indirect, occurring through fibrous connections or muscular stumps.[1] The direct defect, more often present in the septal leaflet (SL) although with variable extent, leads to the separation between the anatomical and functional TV annulus, resulting in an atrialised portion of the RV (aRV). Consequently, EA is not a single disease but rather a spectrum,

marked by substantial structural and clinical variability among affected patients.[1]

The two most widely used classification systems for assessing EA severity are the Carpentier classification (CC) and the Great Ormond Street Echocardiography (GOSE) score, both introduced in the early 1990s.[2 3] The CC categorises EA into four types based on visual assessment of the degree of TV displacement and RV atrialisation. Type A represents the mildest form, characterised by limited impairment of the SL and inferior leaflet (IL), a small aRV and a well-preserved functional RV (fRV). Types B and C display progressively more severe abnormalities, with type C also exhibiting a partial restriction in the motion of the anterior leaflet (AL) and significant fRV dysfunction. Type D, the most severe form, is defined by complete adherence of SL and IL to the RV wall, at least partial adherence of AL, marked enlargement of aRV and a fRV limited to the infundibulum.[2] The GOSE score offers the benefit of quantitatively assessing EA severity; however, it has been originally described on two-dimensional (2D) echocardiographic measurements and it has been demonstrated a prognostic correlation only in neonates.[3] Cardiovascular MR (CMR) provides an unrestricted view of the right-sided cardiac chambers, even in adolescents and adults, who may present suboptimal acoustic windows.[4 5] These age groups often fall within a clinical 'grey zone' where decisions regarding surgical intervention are challenging, underscoring the need for a comprehensive evaluation of both ventricles and TV anatomy.[1]

Current standard surgical EA treatment involves delaminating all the TV tissue adherent to the RV endocardium and reconstructing a 360° cone of valve tissue, which is then sutured to the anatomical TV annulus, hence the name 'cone repair' (CR).[6] Although this technique has shown excellent results in achieving neo-TV competence, a consistent improvement in RV systolic function has yet to be demonstrated; this may influence both patient selection and decisions regarding additional surgical modifications.[1 7] This concept aligns with the growing understanding that EA is more than a valvular disease, as it affects both right and left ventricular structure and function.[1 7–10]

In a population diagnosed with EA, the present study aimed to: (1) evaluate the association of CMR parameters with CC and heart failure (HF) symptoms; (2) determine whether CMR-derived markers can predict the need for bidirectional cavopulmonary anastomosis (BCPA), haemodynamic complications in the early postoperative course and significant right ventricle dysfunction (RVD) following TV surgery.

METHODS

Study population

The study retrospectively enrolled patients diagnosed with EA who underwent a CMR examination at IRCCS Policlinico San Donato between January 2020 and September 2024.

A direct delamination defect of the SL with an apical displacement of its hinge point ≥8 mm/m² from the anterior leaflet of the mitral valve was established as an EA diagnostic criterion.[1 5] Patients with other forms of TV dysplasia, previous TV surgery or poor image quality were excluded. Clinical data were retrieved from hospital databases.

CMR postprocessing

CMR examinations were performed using a 1.5T MAGNETOM Aera (Siemens Healthcare, Erlangen, Germany) scanner. CMR images were analysed blinded to clinical evidence; acquisition protocol, scan parameters and reproducibility data are detailed in the online supplemental material. Ventricular volumes were calculated from short-axis cine steady-state free precession sequences (SSFP) using a thresholding method with Medis software (QMass, V.6.2.1, Medis Medical Imaging Systems, Leiden, The Netherlands) and a constant cross-referencing with all available long-axis ventricular views. The TV regurgitation fraction was calculated as the difference between fRV stroke volume and total forward flow in the pulmonary artery, divided by fRV stroke volume.[11] The presence of IL direct delamination defects (ILd) and late gadolinium enhancement was visually assessed. Severity indices were calculated from cine-SSFP images as schematised in figure 1.[5 12–16] The inferior leaflet displacement (ILD) was measured at end-systole as the distance between the anatomical TV annulus and the inferior leaflet hinge point on a cine-SSFP vertical RV long axis view. When the defect of delamination was complete, the total length of the atrialised wall was considered. The ratio between the aRV and fRV over the anatomical RV (ARV) was calculated using both end-diastolic ventricular volumes (aRV/ARV_{3D}, fRV/ARV_{3D}) and end-systolic long axis assessed in four-chamber view (aRV/ARV_{2D}, fRV/ARV_{2D}). Other indices were calculated according to existing literature.[5 12–16] The Celermajer index was calculated using both end-systolic areas (Cel_{2D}) and end-diastolic volumes (Cel_{3D}).[14 15] Linear measurements and volumes were indexed to body surface area according to the DuBois method.

Study endpoints

CC was assessed visually using CMR and confirmed through direct visual inspection in the operation room for patients who underwent TV surgery. Based on the symptoms reported at the time of CMR, patients were classified according to the New York Heart Association (NYHA) class.[17] For patients hospitalised for TV surgery, transthoracic echocardiography (TTE) was evaluated on admission and at discharge. TR and RVD were assessed with the use of a 5-point semiquantitative scale (absent, mild, mild-to-moderate, moderate, moderate-to-severe, severe) due to the inherent limitations of quantitative measurements.[18] Patients who underwent surgical

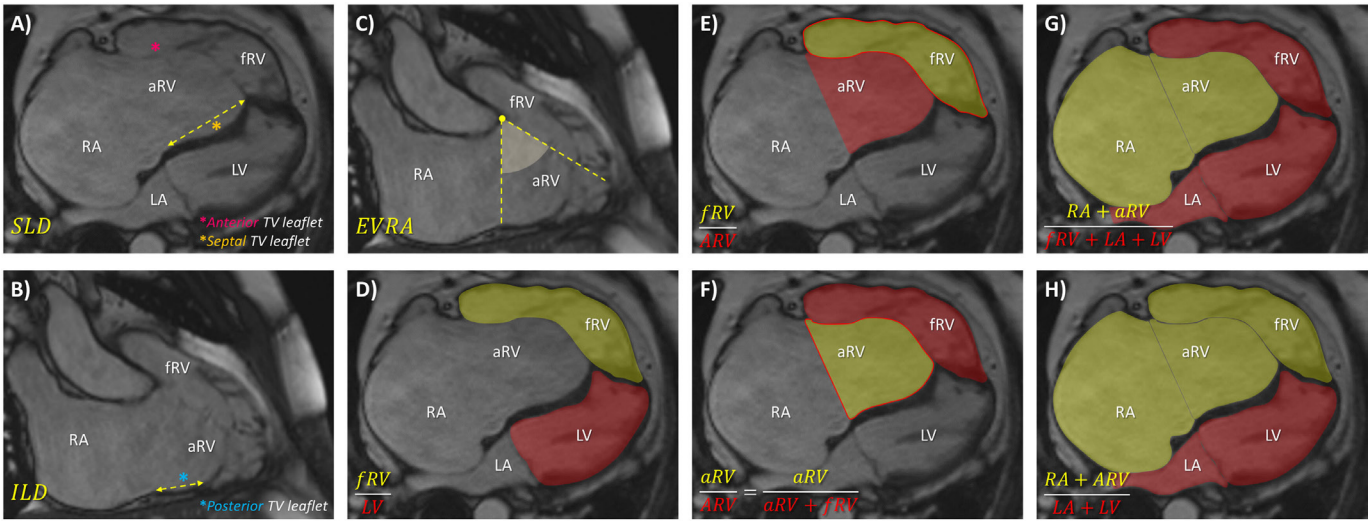

Figure 1 Quantitative CMR-derived indices of disease severity in EA. Cine steady-state free precession sequences showing: (A) septal leaflet displacement; (B) inferior leaflet displacement; (C) Ebstein's valve rotation angle (EVRA); (D) fRV/LV; (E) fRV/ARV; (F) aRV/ARV; (G) Celermajer index (Cel); (H) total right/left-volume index. aRV, atrialised right ventricle; ARV, anatomical right ventricle; CMR, cardiovascular MR; EA, Ebstein's Anomaly; fRV, functional right ventricle; RA, right atrium; LA, left atrium; LV, left ventricle.

intervention were dichotomised based on whether they (1) received a BCPA in conjunction with TV surgery; (2) experienced haemodynamic complications during the postoperative course, defined as hypotension (systolic blood pressure <90 mm Hg or a drop by 40% from baseline levels) persisting despite intravenous fluid administration for more than 30 minutes and (3) had significant RVD at discharge, defined as moderate, moderate-to-severe or severe as assessed by TTE. A BCPA was performed after excluding elevated left-sided heart pressure in cases where RV function was deemed significantly depressed, or—following repair—in cases of failure to wean from cardiopulmonary bypass (CBP), elevated right atrial pressures or significant TV stenosis (mean gradient >5 mm Hg). Further details are available in the section 'Surgical technique' of the online supplemental material.

Statistical analysis

Statistical analyses were performed using SPSS V.28.0 (IBM). Normality was assessed with the Shapiro-Wilk test. Continuous variables are reported as mean±SD or median and IQR depending on distribution, with group comparisons made using Student's t-test or Mann-Whitney U test. Differences across Carpentier classes were analysed using ANOVA or Kruskal-Wallis test, followed by post hoc pairwise comparisons without formal adjustment for multiple comparisons. Multinomial logistic regression assessed associations between CMR parameters and Carpentier classes, while receiver operating characteristic (ROC) curve analysis evaluated CMR predictive value for EA severity (area under the curve and Youden Index for cut-off). Logistic regression models explored predictors of NYHA ≥II, BCPA need, haemodynamic complications in the early postoperative course and significant RVD at discharge, with $p<0.05$ deemed significant.

RESULTS

Study population

The study included 60 patients (32 males; 53%) with a median age of 22 years old (IQR 12, 41). Most patients were classified with a type C anatomy (n=25, 42%), followed by type B (n=17, 28%), type A (n=11, 18%) and type D (n=7, 12%). Online supplemental materials contain further details on study population (paragraph 'Patient Population') and clinical decision-making (online supplemental figure 1).

Among the 60 patients included in the study, 30 underwent TV surgery: 27 (90%) received CR while 3 (10%) underwent TV replacement. BCPA was performed in nine patients (seven with type C and two with type D anatomies).

Haemodynamic complications occurred in nine patients following TV surgery (30%). Two patients left the operating room with open chest; one of them required extracorporeal membrane oxygenation support and died 19 days later due to multiple organ dysfunction. Among the remaining seven patients, haemodynamic complications occurred in intensive care unit and were associated with sustained arrhythmias, including bradyarrhythmias requiring temporary pacing (n=2), junctional tachycardia (n=2), ventricular tachycardia (n=1) and sustained atrial fibrillation (n=2). Two patients experienced early cone breakdown requiring reoperation, one due to rupture of the neo-chordae placed at the postero-septal commissure and the other due to detachment of the pericardial patch used for IL augmentation.

At hospital discharge, all the patients showed an improvement in TV regurgitation (TR) improvement compared with admission (online supplemental figure 2). RVD at discharge was graded as mild in 4 patients

Table 1 Baseline characteristics and quantitative CMR indices of EA severity

Variable	Total (n=60)	Carpentier classification				P value
		A (n=11)	B (n=17)	C (n=25)	D (n=7)	
Age, years	22 (12, 41)	15 (11, 42)	23 (14, 35)	28 (12, 45)	21 (11, 37)	0.87
Male, n (%)	32 (53.3)	6 (54.5)	10 (58.8)	12 (48.0)	4 (57.1)	0.91
Arrhythmic history, n (%)	17 (28.3)	0 (0.0)	4 (23.5)	7 (28.0)	6 (85.7)	**0.001**
NYHA≥II	21 (35.0)	0 (0.0)	6 (35.3)	10 (40.0)	5 (71.4)	**0.02**
BSA, kg/m^2	1.61±0.42	1.54±0.42	1.62±0.35	1.63±0.46	1.62±0.53	0.95
HR, bpm	72 (60, 82)	70 (64, 93)	67 (60, 79)	72 (59, 83)	73 (53, 78)	0.66
aRV EDVi, mL/m^2	48.3 (29.0, 69.6)	18.8 (10.3, 46.8)$^{C, D}$	31.3 (24.0, 61.1)^{D}	55.0 (38.5, 75.8)	92.4 (43.5, 156.6)	**0.001**
ARV EDVi, mL/m^2	164.9 (140.8, 219.1)	157.9 (126.3, 182.1)	156.2 (119.1, 177.5)	179.5 (153.2, 240.4)	258.2 (132.7, 31.1)	0.05
fRV EDVi, mL/m^2	123.4 (95.1, 60.5)	117.5 (101.9, 162.3)	102.9 (92.0, 137.3)	129.1 (98.6, 174.2)	159.6 (84.4, 174.6)	0.42
fRV ESVi, mL/m^2	57.7 (47.8, 89.8)	49.6 (41.0, 78.5)	57.3 (38.1, 74.4)	59.7 (51.2, 107.2)	88.5 (51.1, 110.3)	0.08
fRV MI, g/m^2	20.1 (22.3, 39.0)	30.7 (24.8, 50.7)	24.1 (20.6, 30.1)	25.0 (21.5, 41.0)	28.9 (22.2, 40.6)	0.18
fRV EF, %	47.4 (39.5, 55.9)	57.7 (54.8, 58.5)^{C,D}	47.9 (43.8, 54.7)	46.1 (38.4, 56.0)	38.3 (30.9, 41.8)	**0.001**
LV EDVi, mL/m^2	63.7 (54.1, 69.6)	62.0 (57.4, 68.6)	65.6 (53.6, 71.6)	60.8 (49.1, 72.6)	67.3 (57.1, 75.2)	0.73
LV ESVi, mL/m^2	24.3 (19.3, 28.8)	21.3 (17.9, 28.6)	24.0 (19.2, 29.2)	22.8 (19.2, 28.3)	25.9 (25.5, 28.9)	0.13
SV, mL	64 (46, 78)	61 (49, 79)	64 (54, 74)	64 (38, 78)	46 (44, 82)	0.93
CO, L/min	4.1 (3.2, 5.4)	3.9 (3.2, 5.8)	4.5 (3.8, 5.6)	4.2 (2.9, 5.1)	4.0 (2.8, 4.2)	0.66
CI, L/min/m^2	2.8 (2.1, 3.5)	2.9 (2.6, 3.6)	2.8 (2.4, 3.4)	2.6 (2.0, 3.5)	2.1 (1.7, 3.6)	0.37
LV MI, g/m^2	53.1 (39.6, 59.3)	53.2 (43.3, 59.5)	53.7 (39.6, 67.8)	49.7 (38.6, 57.6)	54.4 (49.5, 59.8)	0.62
LV EF, %	61.4±8.0	65.0±6.4^{D}	62.5±6.0	60.9±8.7	55.7±9.9	**0.04**
LV NCF, n (%)	23 (38.3)	2 (18.2)	6 (35.3)	11 (44.0)	4 (57.1)	0.32
TV RF, %	39.6±19.0	39.5±21.1	34.7±18.4	43.9±18.3	36.3±20.4	0.44
ATV AP, mm	49 (39, 60)	41 (33, 48)^{C}	42 (39, 51)	57 (48, 62)	50 (33,61)	**0.02**
ATV SI, mm	47 (40, 54)	50 (41, 53)	44 (39, 49)	47 (41, 57)	45 (43, 61)	0.67
RA ESVi, mL/m^2	82.7 (64.1, 118.7)	70.1 (61.7, 107.7)	77.3 (54.6, 105.3)	103.5 (76.3, 165.1)	98.0 (69.4, 141.5)	0.19
SLD, mm	37 (25, 50)	20 (17, 24)$^{C, D}$	38 (25, 45)	38 (28, 55)	50 (46, 76)	**<0.001**
SLDi, mm/m^2	24.2 (16.8, 29.7)	12.2 (9.6, 22.4)^{C,D}	23.8 (16.0, 26.3)	27.8 (20.8, 31.4)	38.8 (29.2, 48.7)	**<0.001**
ILd, n (%)	36 (60.0)	0 (0.0)	8 (47.1)	22 (88.0)	6 (85.7)	**<0.001**
ILD, mm	32 (0, 43)	0 (0, 0)$^{C, D}$	18 (0, 38)$^{C, D}$	40 (32, 44)	49 (37, 72)	**<0.001**
ILDi, mm/m^2	19.9 (0.0, 27.3)	0.0 (0.0, 0.0)$^{C, D}$	12.1 (0.0,21.9)^{C,D}	23.0 (20.3, 33.6)	34.0 (27.5, 46.2)	**<0.001**
EVRA, °	54 (8, 72)	0 (0, 0)$^{C, D}$	35 (15, 45)$^{C, D}$	67 (60, 75)	88 (81, 89)	**<0.001**
aRV/AR$_{2D}$, -	0.85 (0.55, 1.32)	0.36 (0.31,0.67)^{B,C,D}	0.86 (0.55, 1.37)	1.07 (0.71, 1.37)	1.78 (1.22, 3.20)	**<0.001**
aRV/ARV$_{3D}$, -	0.29 (0.18, 0.35)	0.13 (0.07, 0.32)^{C,D}	0.27 (0.18, 0.36)^{D}	0.30 (0.21, 0.34)	0.41 (0.34, 0.48)	**0.001**
fRV/ARV$_{2D}$, -	0.52 (0.41, 0.66)	0.67 (0.62, 0.76)^{C,D}	0.58 (0.44, 0.69)	0.47 (0.41, 0.55)	0.37 (0.26, 0.49)	**0.001**
fRV/ARV$_{3D}$, -	0.71 (0.65, 0.82)	0.87 (0.68, 0.93)$^{C, D}$	0.73 (0.65, 0.83)^{D}	0.70 (0.67, 0.79)	0.59 (0.52, 0.66)	**0.001**
fRV/LV, -	1.96 (1.48, 2.69)	2.11 (1.79, 2.45)	1.70 (1.35, 2.05)	2.09 (1.52, 3.14)	2.16 (1.21, 2.80)	0.19
Cel$_{3D}$, -	0.50 (0.37, 0.64)	0.37 (0.19, 0.52)^{D}	0.44 (0.28, 0.60)^{D}	0.54 (0.45, 0.66)	0.78 (0.52, 1.05)	**0.006**
Cel$_{2D}$, -	0.59 (0.49, 0.84)	0.51 (0.35, 0.63)	0.54 (0.45, 0.63)	0.69 (0.52, 0.99)	0.76 (0.56, 1.20)	**0.010**
Total R/L, -	2.98 (2.16, 3.58)	2.64 (1.87, 3.47)	2.34 (1.73, 3.13)^{C}	3.24 (2.49, 3.71)	3.20 (2.10, 5.82)	**0.045**

Continued

Table 1 Continued

Variable	Total (n=60)	Carpentier classification A (n=11)	B (n=17)	C (n=25)	D (n=7)	P value

One-way ANOVA or Kruskal-Wallis test according to data normality for continuous variables and post hoc pairwise comparison between groups of Carpentier classification (B, P value < 0.05 vs. Carpentier class B; C, P value < 0.05 vs. Carpentier class C; D, P value < 0.05 vs. Carpentier class D;); χ^2 test for categorical variables. Statistical significant P values reported in bold.
Subscripts: 2D, based on long axis or, for Cel, on areas; 3D based on volumes.

ANOVA, analysis of variance; aRV, atrialised right ventricle; ARV, anatomical right ventricle; ATV AP, anatomical tricuspid valve annulus measured in anterior-posterior direction; ATV SI, ATV in superior-inferior direction; BSA, body surface area; Cel, Celemajer index; CI, cardiac index; CMR, cardiovascular MR; CO, cardiac output; EA, Ebstein's Anomaly; EDVi, indexed end-diastolic volume; EF, ejection fraction; ESVi, indexed end-systolic volume; EVRA, Ebstein's valve rotation angle; fRV, functional right ventricle; HR, heart rate; ILd, inferior direct leaflet delamination defect; ILDi, indexed inferior leaflet displacement; LV, left ventricle; MI, mass index; NCF, features of myocardial non compaction; NYHA, New York Heart Association class; RA, right atrium; SLDi, indexed septal leaflet displacement; SV, stroke volume; Total R/L, total right over left volumes index.

(14%), mild-to-moderate in 4 (14%), moderate in 13 (45%), moderate-to-severe in 5 (17%) and severe in 3 (10%).

CMR indices across Carpentier Classification

Baseline characteristics across Carpentier classes are

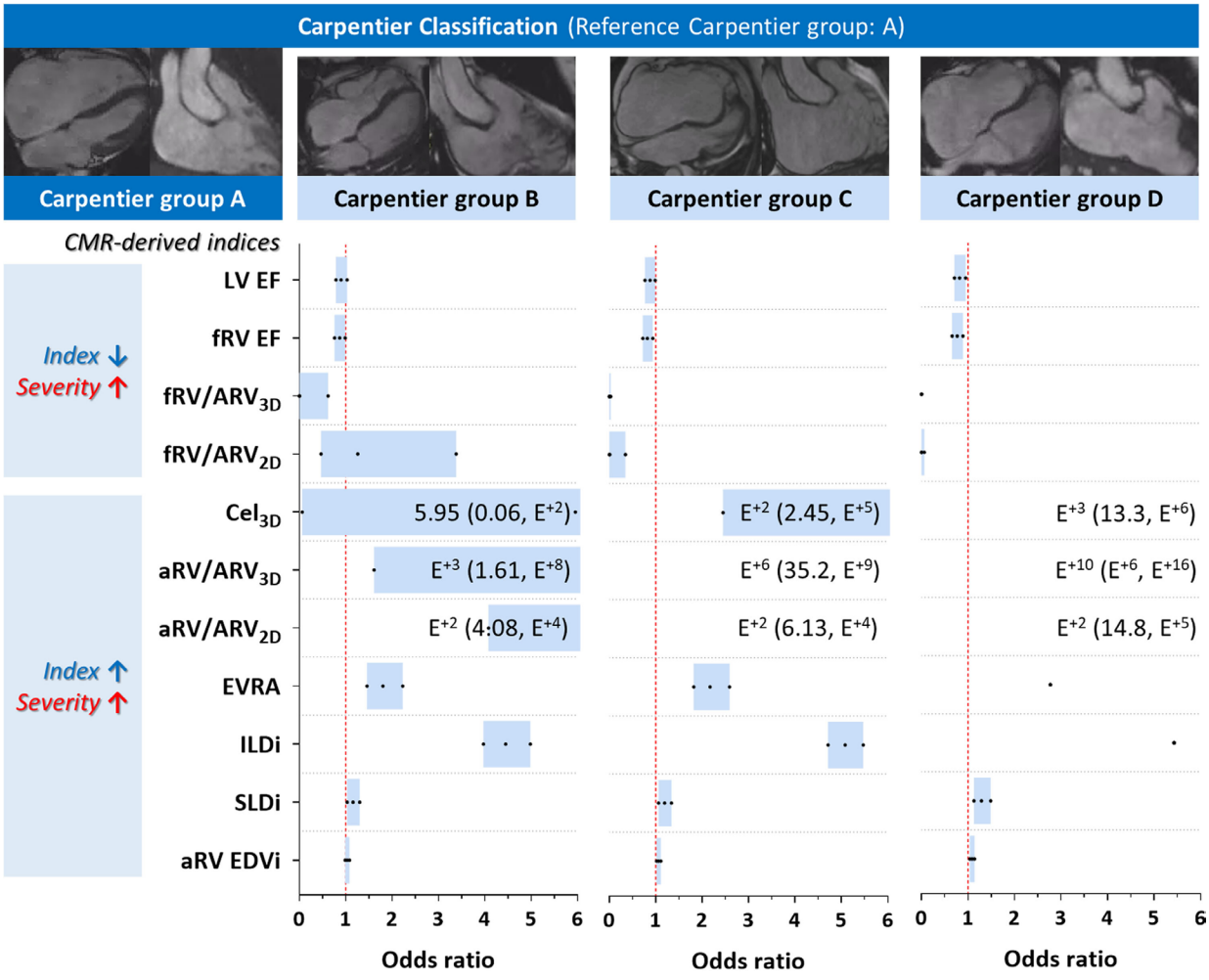

Figure 2 ORs of CMR-derived indices in relation to Carpentier classification. End-systolic balanced cine steady-state free precession sequences of horizontal and vertical right chamber long axis views are shown. 2D, two-dimensional measure based on long axis images; 3D, three-dimensional measure based on volumes; aRV, atrialised right ventricle; ARV, anatomical right ventricle; BCPA, bidirectional cavopulmonary anastomosis; CC, Carpentier classification; Cel, Celermajer index; CMR, cardiovascular magnetic resonance; EA, Ebstein's Anomaly; EDVi, indexed end-diastolic volume; EF, ejection fraction; EVRA, Ebstein valve rotation angle; fRV, functional right ventricle; ILDi, indexed inferior leaflet's displacement; LV, left ventricle; SLDi indexed septal leaflet's displacement.

Table 2 Comparison of baseline characteristics and CMR parameters in relation to the presence of symptoms of heart failure

	HF symptoms			Univariate	
Variables	No **(n=39)**	Yes **(n=21)**	**P value**	**OR (95% CI)**	**P value**
Age, years	20 (13, 41)	28 (13, 42)	0.43	1.02 (0.99, 1.05)	0.31
Male, n (%)	20 (51.3)	12 (57.1)	0.79	1.27 (0.44, 3.69)	0.67
Arrhythmic history, n (%)	7 (17.9)	10 (47.6)	**0.03**	4.16 (1.27, 13.6)	**0.02**
BSA, Kg/m^2	1.63±0.41	1.57±0.46	0.58	0.69 (0.20, 2.44)	0.57
HR, bpm	70 (57, 83)	73 (65, 82)	0.41	1.02 (0.98,1.05)	0.35
aRV EDVi, mL/m^2	42.7 (29.3, 57.9)	63.1 (26.4, 85.0)	0.07	1.02 (0.99, 1.03)	0.08
ARV EDVi, mL/m^2	157.9 (132.7, 182.1)	206.5 (159.2, 266.6)	**0.03**	1.01 (1.01, 1.02)	**0.03**
fRV EDVi, mL/m^2	115.9 (94.7, 138.7)	143.1 (104.1, 178.2)	0.08	1.01 (0.99, 1.02)	0.08
fRV ESVi, mL/m^2	54.5 (42.9, 68.2)	76.2 (51.7, 112.9)	**0.02**	1.02 (1.00, 1.04)	**0.02**
fRV MI, g/m^2	25.0 (22.7, 31.4)	31.8 (22.2, 44.1)	0.15	1.02 (0.99, 1.06)	0.24
fRV EF, %	54.7 (41.8, 57.8)	43.6 (35.4, 52.0)	**0.005**	0.92 (0.87, 0.98)	**0.007**
LV EDVi, mL/m^2	65.1±13.0	58.9±13.9	0.09	0.96 (0.92, 1.01)	0.09
LV ESVi, mL/m^2	23.2±6.9	25.3±6.8	0.27	1.05 (0.97, 1.13)	0.27
SV, mL	69.3±24.6	51.7±19.9	**0.007**	0.96 (0.94, 0.99)	**0.01**
CO, L/min	4.4 (3.6, 5.6)	3.8 (2.6, 4.4)	**0.01**	0.56 (0.35, 0.91)	**0.02**
CI, L/min/m^2	3.0±0.7	2.5±0.8	**0.02**	0.41 (0.19, 0.90)	**0.03**
LV MI, g/m^2	52.4±13.9	52.2±10.8	0.95	1.00 (0.96, 1.04)	0.95
LV EF, %	64.8±5.7	56.4±9.6	**0.001**	0.86 (0.78, 0.94)	**0.001**
LV NCF, n (%)	14 (35.9)	9 (42.9)	0.78	1.29 (0.43, 3.81)	0.65
TV RF, %	37.7±16.2	43.7±22.5	0.24	1.02 (0.99, 1.05)	0.24
ATV AP, mm	48.2±10.7	50.6±12.6	0.45	1.02 (0.97, 1.07)	0.44
ATV SI, mm	45.7±8.0	51.2±14.1	0.12	1.05 (0.99, 1.11)	0.08
RA ESVi, mL/m^2	80.7 (61.8, 109.3)	84.6 (68.4, 193.5)	0.07	1.01 (1.00, 1.03)	**0.01**
SLD, mm	36.3±16.8	43.3±17.4	0.13	1.03 (0.99, 1.06)	0.14
SLDi, mm/m^2	4 (13.9, 28.9)	25.5 (23.2, 40.3)	**0.05**	1.05 (1.00, 1.11)	**0.05**
ILd, n (%)	19 (48.7)	17 (81.0)	**0.03**	4.47 (1.27, 15.7)	**0.02**
ILD mm	21 (0, 42)	37 (30, 54)	**0.02**	1.04 (1.01, 1.07)	**0.01**
ILDi, mm/m^2	12.9 (0.0, 24.0)	24.7 (17.8, 36.8)	**0.008**	1.06 (1.02, 1.11)	**0.007**
EVRA, °	45 (0, 67)	63 (40, 78)	**0.02**	1.03 (1.01, 1.05)	**0.02**
aRV/ARV_{2D}, -	0.73 (0.47, 1.22)	1.09 (0.83, 1.92)	**0.03**	1.58 (0.82, 3.06)	0.18
aRV/ARV_{3D}, -	0.26±0.12	0.30±0.13	0.22	17.6 (0.18, E^3)	0.22
fRV/ARV_{2D}, -	0.58 (0.42, 0.71)	0.47 (0.37, 0.54)	**0.04**	0.03 (0.00, 1.17)	0.06
fRV/ARV_{3D}, -	0.74±0.12	0.70±0.13	0.22	0.06 (0.00, 5.55)	0.22
fRV/LV, -	1.88 (1.46, 2.26)	2.72 (1.50, 3.44)	**0.03**	2.23 (1.13, 4.41)	**0.02**
Cel_{3D}, volumes	0.49 (0.33, 0.62)	0.57 (0.42, 0.78)	0.12	7.02 (0.77, 63.7)	0.08
Cel_{2D}, areas	0.56 (0.49, 0.71)	0.64 (0.49, 0.98)	0.27	2.25 (0.47, 10.9)	0.31
Total R/L, -	2.68 (1.97, 3.22)	3.57 (2.31, 4.60)	**0.03**	1.61 (1.03, 2.53)	**0.04**
LGE*, n/N_{av} (%)	9/34 (26.5)	4/13 (30.8)	1.00	1.24 (0.30, 5.02)	0.77

Mann-Whitney U test for all continuous variables; χ^2 test for categorical variables. Statistical significant P values reported in bold.
Subscripts: 2D, based on long axis or, for Cel, on areas; 3D based on volumes.
*LGE not available for all patients.
AP, anterior–posterior; aRV, atrialised right ventricle; ARV, anatomical right ventricle; ATV, anatomical tricuspid valve annulus; BSA, body surface area; Cel, Celemajer index; CI, cardiac index; CMR, cardiovascular MR; CO, cardiac output; EDVi, indexed end-diastolic volume; EF, ejection fraction; ESVi, indexed end-systolic volume; EVRA, Ebstein's valve rotation angle; fRV, functional right ventricle; HR, heart rate; ILd, inferior leaflet direct delamination defect; ILD, inferior leaflet displacement; ILDi, indexed ILD; LGE, late gadolinium enhancement; LV, left ventricle; MI, mass index; NCF, features of myocardial non compaction; RA, right atrium; SI, superior-inferior; SLD, septal leaflet displacement; SLDi, indexed septal leaflet displacement; SV, stroke volume; Total R/L, total right over left volumes index; TV, tricuspid valve.

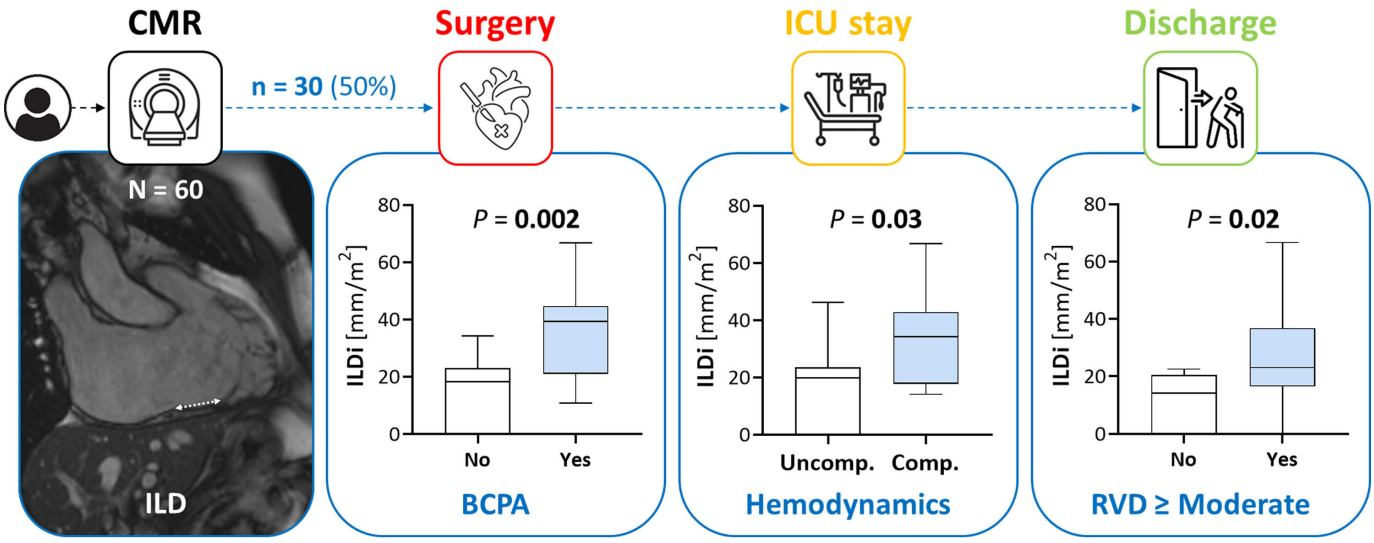

Figure 3 Potential role of indexed inferior leaflet displacement (ILDi, i.e., ILD indexed to BSA) in EA surgical planning. End-systolic balanced cine steady-state free precession sequences of vertical right-ventricular long axis view are shown. BCPA, bidirectional cavopulmonary anastomosis; CMR, cardiovascular magnetic resonance; Comp., complicated; EA, Ebstein's Anomaly; ICU, intensive care unit; ILD, inferior leaflet displacement; ILDi, indexed inferior leaflet displacement; RVD, right ventricular systolic dysfunction; Uncomp., uncomplicated.

summarised in table 1 and figure 2. With increasing disease severity, indexed septal and inferior leaflet displacement (SLDi, ILDi) and other markers of RV atrialisation (aRVEDVi, ARVEDVi, aRV/ARV_{2D}, aRV/ARV_{3D}, fRV/ARV_{2D}, fRV/ARV_{3D}, Cel_{3D}) progressively increased, while biventricular ejection fraction (EF) declined.

Type A class showed no ILd and no rotation of the functional annulus toward the RVOT. From class B to D, the prevalence of ILd and extent of ILD, ILDi and Ebstein valve rotation angle (EVRA) increased. All these parameters were significantly associated with CC in multinomial logistic regression online supplemental table 2.

At ROC analysis, EVRA and ILDi reported the highest discriminatory performance for distinguishing the mildest from the most severe anatomical forms (area under the curve of 0.98 and 0.89 and cut-off values of 54° and 17.8 mm/m^2, respectively (online supplemental table 3).

CMR indices in relation to clinical symptoms

Across Carpentier classes, there was a significant increase in the prevalence of arrhythmias and NYHA class ≥II (table 1 and table 2). Patients with HF symptoms were more likely to have a history of arrhythmias and showed lower biventricular EF and cardiac output compared with asymptomatic patients (table 2). They also exhibited higher indices of right-left chamber volume imbalance (fRV/LV and total R/L), greater IL delamination defects (ILD, ILDi, EVRA) and larger right chamber volumes (ARVEDVi, fRV/ARV_{2D}, fRVESVi, table 2). In multivariable logistic regression including LV EF, fRV EF and ILDi, both LV EF (OR 0.85, 95% CI 0.75 to 0.97, p=0.01) and ILDi (OR 1.05, 95% CI 1.00 to 1.10, p=0.04) remained independently associated with HF symptoms.

Exploratory CMR-based findings in relation to surgical outcomes

Three patients, aged 40, 43 and 69 years, underwent TV replacement. They were older than most patients who received CR and had among the highest ILDi (19.8, 32.7 and 42.4 mm/m²) and EVRA (72°, 76° and 80°) values (online supplemental table 4). Additionally, the two patients who experienced early CR failure had preoperative EVRA values of 35° and ILDi values of 22.6 and 23.0 mm/m², respectively.

Online supplemental table 5 compares the CMR characteristics of patients who received BCPA compared with those who maintained a complete biventricular circulation. Among the parameters that differed between the two groups, ILD, ILDi and EVRA showed a tendency towards association with the need for BCPA in univariate analysis.

Regarding postoperative haemodynamic complications (online supplemental table 6), ILd (100% vs 52.4%) and a history of arrhythmias (55.6% vs 14.3%) were more frequent among patients with complications. These patients also showed lower fRV/ARV_{3D} ratios (mean value of 0.65 vs 0.76), and higher ILDi (median of 34.3 vs 19.8), aRV/ARV_{3D} ratio (mean value of 0.35 vs 0.24), Cel_{2D} index (median of 0.94 vs 0.55) and Cel_{3D} index (mean values of 0.68 vs 0.47). In univariate logistic regression analysis, both ILDi (OR 1.09) and arrhythmic history (OR 7.50) showed a trend towards association with postoperative haemodynamic complications.

Finally, ILDi was higher in patients with moderate or severe RV systolic dysfunction at discharge compared with those with milder RVD (median of 14.1 vs 23; online supplemental table 6) and showed a tendency toward association with RVD in univariate analysis (OR 1.08).

These preliminary findings regarding preoperative ILDi in relation to surgical outcomes are illustrated in figure 3.

DISCUSSION

The study identified quantitative CMR-derived markers of structural severity in EA, where this assessment has traditionally been qualitative using CC. The association of specific CMR-derived indices with HF symptoms and—on an exploratory basis—with surgical outcomes may serve as preliminary further support of their link to EA anatomical severity. A classification system based on quantitative rather than qualitative criteria holds the potential to provide a more accurate risk stratification for a personalised monitoring strategy and therapeutic approach in EA.

Quantitative CMR-based assessment in EA

In this study, the parameters most strongly associated with CC were shown to exhibit a marked intercorrelation. The presence of ILd was paralleled by an anterior-superior rotation of the functional TV annulus towards the RVOT, as well as, by increasing indices of RV atrialisation. In patients classified as type A, where the functional TV annulus is only apically displaced, IL abnormalities were absent or limited to indirect focal delamination defects, without measurable ILD or EVRA. With worsening IL impairment from type B to type D, ILd became more frequent, accompanied by rising ILDi and EVRA. Both ILDi and EVRA outperformed SLDi in identifying the most severe anatomies, underscoring the additional value of CMR over TTE, on which most morphological studies have historically relied.[1 3 5]

The finding that ILDi and EVRA were elevated in patients with early cone breakdown is consistent with previous evidence and further advocates that they may serve as indicators of TV structural complexity.[13]

Our results suggest that ILDi may help identify high-risk structural phenotypes, as it was associated with HF symptoms and with the occurrence of post-operative haemodynamic complications. This may be partially explained by the evidence that a greater ILDi was found to parallel an increase in aRV size and TV complexity.[19] The progressive apical displacement of the TV annulus across CC, reflected by rising SLDi and ILDi, may contribute to the escalating prevalence of arrhythmias from type A to D, possibly due to accessory pathways in regions of impaired delamination and enlarged aRV.[1 20 21] However, a clear association between structural severity and sudden death remains to be established.[19 22]

NYHA class was also associated with the right-to-left heart size ratio and with biventricular EF, in line with previous findings.[12 15 16] While progressively declining as EA severity increased, LV EF remained within normal limits for most patients of our cohort. This suggests that it may be considered as a subtle risk factor, since its association with adverse cardiac events is well-known in EA.[1 8 9]

Potential implications for surgical planning

The choice of a BCPA in addition to CR has been generally decided intraoperatively, particularly in cases of difficult weaning from CBP, increased right atrial pressures, or when neo-valve stenosis emerges following significant valve remodelling.[1 23] Consistently, patients who received a BCPA showed lower cardiac output and smaller TV annular dimensions at preoperative CMR compared with patients who received TV surgery in a complete biventricular circulation.

Deciding on a BCPA preoperatively could reduce CBP time and may facilitate a more effective TV repair, potentially improving postsurgical outcomes.

A recent consensus statement from the American Association for Thoracic Surgery highlighted some shared criteria for considering the addition of a BCPA to the TV repair.[24] Alongside the aforementioned intraoperative factors, the document also reported a fRV end-diastolic volume >250 mL/m² or a fRV EF <25% as preoperative findings to be considered for BCPA association with CR.

In the absence of a severe fRV dilation or dysfunction, a relevant clinical question is the ability to anticipate how CR will affect RV performance, given that the procedure entails a true structural remodelling of the chamber.[1] When seeking to anticipate postoperative RVD, it is essential to take into account that CR involves leaflet delamination from myocardial wall and possible aRV resection or plication. Given that the RV systolic mechanism is predominantly based on a longitudinal contraction directed from the inferior wall to the infundibulum, the IL surgical detachment from the myocardial wall may have important consequences on the RV global systolic function after surgery.[25 26] This may help elucidate why higher preoperative ILDi values demonstrated a trend toward an association with more pronounced postoperative RVD. A previous observational study on a similar patient population reported greater prevalence of ILd in subjects who exhibited the worse RV systolic function after surgery.[27]

Further studies are needed to test this hypothesis and to clarify the impact of preoperative ILDi on long-term RVD after CR, particularly in light of the observation that early postoperative dysfunction is often followed by partial recovery during follow-up.[28 29]

Limitations

The presented data reflect the clinical practice of a tertiary care centre team, carrying an inherent risk of selection bias. Its retrospective, single-centre design and limited sample size may reduce statistical power to detect subtle group differences and limit the generalisability of the findings. Additionally, due to the retrospective nature of data collection, certain covariates—such as objective markers of HF—were not consistently available for analysis. For instance, cardiopulmonary exercise testing was not available at baseline for all patients—partly because several underwent CMR during the COVID-19

pandemic—and, when available, it was not performed at time points that were sufficiently aligned with the CMR acquisition.

Furthermore, to validate these preliminary observations and enhance their reliability, a future multicentre study involving larger, independent cohorts of patients with EA is warranted. Also, a dedicated prospective study on RV remodelling after CR would be required, ideally assessing patients at standardised postoperative time points.

Nevertheless, the small sample size was considered acceptable given the low prevalence of the disease[1] and the exploratory scope of the study, which was intended to generate hypotheses rather than establish definitive conclusions.

CONCLUSIONS

Several quantitative CMR indices proved effective in distinguishing between Carpentier classes and hold potential value in a CMR-integrated framework for assessing EA severity. Among them, ILDi emerged as a practical, non-invasive measure that could serve as a valuable marker in the pre-surgical planning of EA, potentially guiding individualised surgical strategies and enhancing postoperative risk stratification.

Author affiliations
[1]Pediatric and Congenital Heart Disease Unit, IRCCS Policlinico San Donato, San Donato Milanese, Italy
[2]PhD Degree Program in Cardio-Nephro-Thoracic Sciences, University of Bologna, Bologna, Italy
[3]3D and Computer Simulation Laboratory, IRCCS Policlinico San Donato, San Donato Milanese, Italy
[4]Department of Electronics, Information and Bioengineering, Politecnico di Milano, Milan, Italy
[5]Multimodality Imaging Cardiac Section, IRCCS Policlinico San Donato, San Donato Milanese, Italy
[6]Postgraduate School in Radiodiagnostics, Università degli Studi di Milano, Milan, Italy
[7]Department of Congenital Cardiac Surgery, IRCCS Policlinico San Donato, San Donato Milanese, Italy
[8]Norfolk and Norwich University Hospitals NHS Foundation Trust, Norwich, UK
[9]Arrhythmia and Electrophysiology Department, IRCCS Policlinico San Donato, San Donato Milanese, Italy
[10]Institute of Molecular and Translational Cardiology (IMTC), San Donato Milanese, Italy
[11]Unit of Radiology, IRCCS Policlinico San Donato, San Donato Milanese, Italy
[12]Faculty of Medicine and Surgery, Vita-Salute San Raffaele University, Milan, Italy
[13]Department of Medical and Surgical Sciences, University of Bologna, Bologna, Italy
[14]Department of Cardio-Thoracic and Vascular Medicine, IRCCS Azienda Ospedaliero-Universitaria di Bologna, Bologna, Italy

Acknowledgements The authors thank the cardiac imaging technical and nursing staff for their dedicated work and Dr Laura Schianchi for her assistance in the role of Clinical Research Coordinator. The support of the European Reference Network for Rare and Low Prevalence Complex Diseases of the Heart (ERN GUARD-Heart, Amsterdam, Netherlands) is gratefully acknowledged. This work was partially supported by Ricerca Corrente funding from Italian Ministry of Health to IRCCS Policlinico San Donato.

Contributors GP conceptualised the research, provided the data and drafted the initial manuscript, coordinating the revision process. FS performed the statistical analysis, supported formal analysis and contributed to the conceptualisation. BC, LT, MA, FB, EM and FT contributed to data collection, curation and validation. MH, ML, EM, PS, CP, EA, MC and AG critically reviewed the intellectual content of the manuscript and provided clinical advice. GP and FS designed, drafted and revised all figures and tables. MC and AG contributed to funding acquisition. All authors revised, contributed to and approved the final version of the manuscript.

Funding This study was funded by Ministero della Salute (Ricerca Corrente).

Competing interests None declared.

Patient consent for publication Not applicable.

Ethics approval The study conformed to the Good Clinical Practice and Declaration of Helsinki principles, and it was approved by the local Ethics Committee (research protocol 'EA-CMR', Comitato Etico Territoriale Lombardia 1, study registration number CET 169-2025). Informed consent was waived due to the retrospective nature of the study and the analysis of anonymised data.

Provenance and peer review Not commissioned; externally peer reviewed.

Data availability statement Data are available on reasonable request. The data that support the findings of this study will be available from the corresponding author on reasonable request.

ORCID iDs
Francesco Sturla https://orcid.org/0000-0001-7317-304X
Massimo Chessa https://orcid.org/0000-0001-7432-4815

REFERENCES

1 Pasqualin G, Boccellino A, Chessa M, *et al*. Ebstein's anomaly in children and adults: multidisciplinary insights into imaging and therapy. *Heart* 2024;110:235–44.
2 Carpentier A, Chauvaud S, Macé L, *et al*. A new reconstructive operation for Ebstein's anomaly of the tricuspid valve. *J Thorac Cardiovasc Surg* 1988;96:92–101.
3 Celermajer DS, Cullen S, Sullivan ID, *et al*. Outcome in neonates with Ebstein's anomaly. *J Am Coll Cardiol* 1992;19:1041–6.
4 Leiner T, Bogaert J, Friedrich MG, *et al*. SCMR Position Paper (2020) on clinical indications for cardiovascular magnetic resonance. *J Cardiovasc Magn Reson* 2020;22:76.
5 Attenhofer Jost CH, Edmister WD, Julsrud PR, *et al*. Prospective comparison of echocardiography versus cardiac magnetic resonance imaging in patients with Ebstein's anomaly. *Int J Cardiovasc Imaging* 2012;28:1147–59.
6 Silva JP JP, Baumgratz JF, Fonseca L, *et al*. The cone reconstruction of the tricuspid valve in Ebstein's anomaly. *The Operation: Early and Midterm Results J Thorac Cardiovasc Surg* 2007;133:215–23.
7 Pasqualin G, Chessa M, Giamberti A. Cardiovascular Magnetic Resonance in decision making for patients with Ebstein anomaly: A call for action. *J Thorac Cardiovasc Surg* 2025;170:e158–9.
8 Inai K, Nakanishi T, Mori Y, *et al*. Left ventricular diastolic dysfunction in Ebstein's anomaly. *Am J Cardiol* 2004;93:255–8.
9 Rydman R, Shiina Y, Diller G-P, *et al*. Major adverse events and atrial tachycardia in Ebstein's anomaly predicted by cardiovascular magnetic resonance. *Heart* 2018;104:37–44.
10 Attenhofer Jost CH, Connolly HM, O'Leary PW, *et al*. Left heart lesions in patients with Ebstein anomaly. *Mayo Clin Proc* 2005;80:361–8.
11 Lancellotti P, Pibarot P, Chambers J, *et al*. Multi-modality imaging assessment of native valvular regurgitation: an EACVI and ESC council of valvular heart disease position paper. *Eur Heart J Cardiovasc Imaging* 2022;23:e171–232.

12 Tobler D, Yalonetsky S, Crean AM, *et al*. Right heart characteristics and exercise parameters in adults with Ebstein anomaly: new perspectives from cardiac magnetic resonance imaging studies. *Int J Cardiol* 2013;165:146–50.
13 Hughes ML, Bonello B, Choudhary P, *et al*. A simple measure of the extent of Ebstein valve rotation with cardiovascular magnetic resonance gives a practical guide to feasibility of surgical cone reconstruction. *J Cardiovasc Magn Reson* 2019;21:34.
14 Cieplucha A, Trojnarska O, Bartczak-Rutkowska A, *et al*. Severity Scores for Ebstein Anomaly: Credibility and Usefulness of Echocardiographic vs Magnetic Resonance Assessments of the Celermajer Index. *Can J Cardiol* 2019;35:1834–41.
15 Yalonetsky S, Tobler D, Greutmann M, *et al*. Cardiac magnetic resonance imaging and the assessment of ebstein anomaly in adults. *Am J Cardiol* 2011;107:767–73.
16 Hösch O, Sohns JM, Nguyen T-T, *et al*. The total right/left-volume index: a new and simplified cardiac magnetic resonance measure to evaluate the severity of Ebstein anomaly of the tricuspid valve: a comparison with heart failure markers from various modalities. *Circ Cardiovasc Imaging* 2014;7:601–9.
17 McDonagh TA, Metra M, Adamo M, *et al*. 2021 ESC Guidelines for the diagnosis and treatment of acute and chronic heart failure: Developed by the Task Force for the diagnosis and treatment of acute and chronic heart failure of the European Society of Cardiology (ESC). With the special contribution of the Heart Failure Association (HFA) of the ESC. *Eur J Heart Fail* 2022;24:4–131.
18 Li W, West C, McGhie J, *et al*. Consensus recommendations for echocardiography in adults with congenital heart defects from the International Society of Adult Congenital Heart Disease (ISACHD). *Int J Cardiol* 2018;272:77–83.
19 Attenhofer Jost CH, Tan NY, Hassan A, *et al*. Sudden death in patients with Ebstein anomaly. *Eur Heart J* 2018;39:1970–1977a.
20 Roten L, Lukac P, DE Groot N, *et al*. Catheter ablation of arrhythmias in ebstein's anomaly: a multicenter study. *J Cardiovasc Electrophysiol* 2011;22:1391–6.
21 Dearani JA, Danielson GK. Congenital Heart Surgery Nomenclature and Database Project: Ebstein's anomaly and tricuspid valve disease. *Ann Thorac Surg* 2000;69:S106–17.
22 Marcondes L, Sanders SP, Del Nido PJ, *et al*. Examination of pathologic features of the right atrioventricular groove in hearts with Ebstein anomaly and correlation with arrhythmias. *Heart Rhythm* 2020;17:1092–8.
23 Quinonez LG, Dearani JA, Puga FJ, *et al*. Results of the 1.5-ventricle repair for Ebstein anomaly and the failing right ventricle. *J Thorac Cardiovasc Surg* 2007;133:1303–10.
24 Chai P, Konstantinov IE, *et al*, Expert Consensus Panel. The American Association for Thoracic Surgery (AATS) 2025 Expert Consensus Document: Management of Ebstein anomaly in children and adults. *J Thorac Cardiovasc Surg* 2025;170:1–16.
25 Kovács A, Lakatos B, Tokodi M, *et al*. Right ventricular mechanical pattern in health and disease: beyond longitudinal shortening. *Heart Fail Rev* 2019;24:511–20.
26 Pasqualin G, Riva A, Sturla F, *et al*. Intracavitary blood flow dynamics in the systemic right ventricle after atrial switch operation: a shift from transverse to longitudinal systolic pattern. *Int J Cardiovasc Imaging* 2025;41:943–54.
27 Alsaied T, Castrillon CD, Christopher A, *et al*. Cardiac MRI predictors of right ventricular dysfunction after the Da Silva cone operation for Ebstein's anomaly. *Int J Cardiol Congenit Heart Dis* 2022;7:100342.
28 Sundaram K, Stoll V, Da Fonseca Da Silva L, *et al*. Mid-Term Recovery of Right Ventricular Function and Improvement of Left Ventricular Function After Da Silva Cone Procedure for Ebstein Anomaly. *J Cardiovasc Dev Dis* 2025;12:276.
29 Anderson HN, Dearani JA, Said SM, *et al*. Cone reconstruction in children with Ebstein anomaly: the Mayo Clinic experience. *Congenit Heart Dis* 2014;9:266–71.